

Calculation of Transition State Energies in the HCN-HNC Isomerization with an Algebraic Model

Jamil Khalouf-Rivera,[†] Miguel Carvajal,^{†,¶} Lea F. Santos,[‡] and Francisco Pérez-Bernal^{*,†,¶}

[†]*Depto. de Ciencias Integradas y Centro de Estudios Avanzados en Física, Matemáticas y Computación, Universidad de Huelva, Huelva 21071, SPAIN*

[‡]*Department of Physics, Yeshiva University, New York, New York 10016, USA*

[¶]*Instituto Carlos I de Física Teórica y Computacional, Universidad de Granada, Granada 18071, SPAIN*

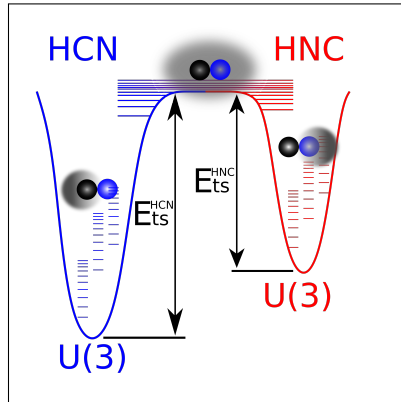
E-mail: curropb@uhu.es

Phone: +34 959219789. Fax: +34 959219777

Abstract

Recent works have shown that the spectroscopic access to highly-excited states provides enough information to characterize transition states in isomerization reactions. Here, we show that the transition state of the bond breaking HCN-HNC isomerization reaction can also be achieved with the two-dimensional limit of the algebraic vibron model. We describe the system's bending vibration with the algebraic Hamiltonian and use its classical limit to characterize the transition state. Using either the coherent state formalism or a recently proposed approach by Baraban *et al.* [*Science* **2015**, *350*, 1338], we obtain an accurate description of the isomerization transition state. In addition, we show that the energy level dynamics and the transition state wave function structure indicate that the spectrum in the vicinity of the isomerization saddle point can be understood in terms of the formalism for excited state quantum phase transitions.

Graphical TOC Entry



Keywords

isomerization transition state, excited state quantum phase transition, two-dimensional vibron model, HCN-HNC isomerization

Transition state theory is considered the keystone of chemical reaction studies and chemical kinetics since its formulation in the 1930's.^{1,2} It allows for the derivation of thermal reaction rates from the energy surface landscape, in particular, from the minimal energy pathway connecting reactants and products. However, the experimental study of transition states is hindered by the saddle structure of the phase space region they inhabit. In recent works, Baraban *et al.*³ and Mellau *et al.*⁴ presented an interesting approach that allows for the characterization of the transition state in isomerization reactions using as an input, spectroscopic data in the frequency domain. The approach in both works is based on a particular spectroscopic pattern: the appearance of a dip in the spacing of adjacent quantum levels for overtone series associated with degrees of freedom that are connected with the reaction coordinate. Baraban *et al.* quantify this dip making use of the *effective frequency*; a quantity defined for quantum systems as $w^{eff}(n) = \frac{\partial E(n)}{\partial n} = \frac{\Delta E}{\Delta n}$, i.e. the discrete derivative of the system energy with respect to the principal quantum number n .^{3,4} They suggest a simple formula³ to parameterize the dependence of the effective frequency on the midpoint vibrational energy \overline{E}

$$w^{eff}(\overline{E}) = \omega_0 \left(1 - \frac{\overline{E}}{E_{TS}}\right)^{\frac{1}{m}}, \quad (1)$$

with three adjustable parameters: ω_0 , m , and E_{TS} . The parameter ω_0 is the effective frequency for the potential ground state and m depends on the potential shape.³ The most relevant parameter is E_{TS} , the transition state energy, which provides an estimate of the energy barrier between different reactants. This formalism was applied in Ref.³ to the vibrational bending spectrum of two isomerizing systems that have been subject to extensive theoretical and experimental analyses: the HCN-HNC bond breaking system and the *cis-trans* configurations in the acetylene S_1 electronic state. In both cases, it was shown how the proposed method helps to identify isomerization pathways, allowing for the distinction between spectator vibrational modes and those particular combinations of modes that favor the isomerization reaction path. In the first case, they were also able to extract a value of

E_{TS} which is within 1% of the value of the isomerization barrier obtained with sophisticated *ab initio* calculations.^{5–7}

In the present work, we show that the algebraic vibron model, provided with enough spectroscopic information, can also be used to characterize the transition state with great accuracy. The vibron model was introduced by Iachello in the 1980’s. It is an algebraic model for molecular structure that treats rovibrational excitations as bosonic particles (vibrons).⁸ The two-dimensional limit of the vibron model (2DVM) is specially tailored for the treatment of bending dynamics.^{9–11} Despite its apparent simplicity, the 2DVM encompasses in a common framework the two limiting physical cases of interest, rigidly-linear and rigidly-bent configurations, as well as the feature-rich non-rigid case, with particular spectroscopic signatures due to the existence of a barrier to linearity.¹⁰ In the non-rigid case, the adjacent quantum level splittings reach a minimum value once anharmonicity switches from negative to positive values. This feature is known as the Dixon’s dip¹² and it was explained by the qualitative change in the system phase space configuration that happens once the system energy reaches the local potential maximum, at the top of the barrier to linearity.¹³ The classical or mean-field limit of the 2DVM¹⁴ can be obtained with the coherent (or intrinsic) state formalism,^{15,16} which provides an exact energy functional in the large system size limit.

By conveniently parameterizing the 2DVM Hamiltonian, the system ground state evolves from a rigidly-linear to a rigidly-bent configuration through the variation of a control parameter. In this process, the ground state undergoes a particularly abrupt change at a critical value of the control parameter. This sudden change has been interpreted as a quantum phase transition,¹⁴ a zero-temperature phase transition purely due to quantum fluctuations, in the same fashion as in other many-body bosonic systems.¹⁷ More recently, this concept was extended to the realm of excited states with excited state quantum phase transitions (ESQPTs), that are characterized by a singularity (in the mean field limit) in the system local density of states at a critical energy value that defines a separatrix between states of different character.^{18,19} ESQPT precursors have been identified in the vibrational bending

spectra of several molecular species and have been associated with the existence of a barrier to linearity in the energy potential through the intrinsic state formalism.^{20,21} The singularity in the spectrum happens once the system energy approaches the top of the barrier, which is marked by a pronounced decrease in level distance. The particular spectroscopic features that appear at such energies were explained introducing the concept of quantum monodromy.^{13,22} The development of new techniques has made it possible to access experimentally excited vibrational states at energies beyond the barrier to linearity.^{23,24} Quantum monodromy can be interpreted as an ESQPT in the 2DVM^{14,19} and the first experimental confirmation of ESQPT spectral signatures took place in the vibrational bending spectra of non-rigid molecular species.^{20,21} Other experimental systems where ESQPT signatures have been identified are superconducting microwave billiards²⁵ and spinor Bose-Einstein condensates.²⁶

In contrast to what happens for molecular dissociation, the dip in the effective frequency value for the HCN-HNC system is explained in terms of a saddle point (or local maximum) in the potential energy surface (PES). This picture holds for both isomerizing and nonrigid molecular species. In the first case, the critical point is associated with the transition state saddle point,^{3,4} while in the second case, it is connected with the top of the barrier to linearity.^{20,21,27} The questions addressed here are whether the 2DVM can be of help in the estimation of the transition state properties from spectroscopic data and if the decrease in the separation between energy levels could be understood as a new example of ESQPT.

To cast light upon these two aspects, we analyze the available data for the HCN-HNC system. The available experimental data for the bending vibrational spectrum of HNC and HCN were already successfully modeled with a four-parameter 2DVM spectroscopic Hamiltonian, which is the most general Hamiltonian including one- and two-body interactions.²¹ Unfortunately, experimental data are not available above 10 000 cm⁻¹ and the dissociation barrier is expected to lie around 17 000 cm⁻¹ above the HCN minimum, which is located approximately 5200 cm⁻¹ below the HNC minimum. To overcome this obstacle, we adopt the same approach taken by Baraban *et al.*³ We use for our calculations a set of *ab initio*

term values⁵ spectroscopically assigned after an exhaustive analysis of the full experimental rovibrational spectrum for the [H,C,N] system.^{6,7} In the present work, selecting the pure bending levels, we consider 142 energies with vibrational angular momenta up to $\ell = 12$ in the case of HCN, compared to 30 available experimental terms, and 41 energy level up to $\ell = 9$ in the case of HNC, compared to only 19 experimental levels.

To reproduce the bending spectrum of the two species, we use the algebraic Hamiltonian

$$\hat{H} = P_{11}\hat{n} + P_{21}\hat{n}^2 + P_{22}\hat{\ell}^2 + P_{23}\hat{W}^2 + P_{45} \left[\hat{W}^2\hat{n}^2 + \hat{n}^2\hat{W}^2 \right], \quad (2)$$

extending the one- and two-body Hamiltonian, employed in²¹ with a four-body operator that is needed to improve the HCN data fit. We obtain the optimized spectroscopic parameter values in Tab. 1 (see supplementary text for details of the fits) through an iterative non-linear least-square fitting procedure that uses the Fortran version of **Minuit**.²⁸

Once we optimize the free parameter values in the spectroscopic Hamiltonian (2), we compute the vibrational bending energy functional for both HCN and HNC, using the intrinsic state formalism^{14,20,21} (see supplementary material for further details). The obtained functionals, depicted in Fig. 1a, allow for the estimation of the isomerization barrier height, E_{TS} , which corresponds to the distance between the functional minimum and its asymptotic value. We provide in Tab. 2, in the column labeled 2DVM-I, the resulting E_{TS} values for HCN and HNC.

We also derive the transition state energy employing a second procedure. We use the effective frequencies from the 2DVM predicted term values for both molecular species. These results, for vibrational angular momentum $\ell = 0$, are shown in Fig. 1b, where ω^{eff} is plotted as a function of \bar{E} using blue (orange) circles for the algebraic model results for HCN (HNC). The effective frequency for spectroscopically assigned *ab initio* data is depicted using green squares and the available experimental data are also included as (cyan) crosses. It is clear from this figure that the 2DVM results undergo the expected dip in the effective frequency and that they provide a very good estimate of the height of the isomerization barrier in the

HCN-HNC molecular system. The HNC data are displaced so that the top of the barrier is common for both molecular species, which allows for the estimation of the separation between the HCN and HNC energy minima. We use the effective frequency of the algebraic term values to fit the parameters in the function (1) with the help of the Python LMFIT package,²⁹ and obtain the estimated barrier values in the column of Tab. 2 labeled as 2DVM-II.

Table 1: Optimized spectroscopic parameters P_{ij} (cm⁻¹ units), root mean square deviation rms (cm⁻¹), and vibron number N obtained from the fit to the HCN and HNC *ab initio* data set^{5,7,30} for Hamiltonian (2). For a detailed description of the fitting procedure see the supplementary material.

Molecule	P_{11}	P_{21}	P_{22}	P_{23}	$P_{45} \times 10^4$	N	rms
HCN	2308.3(6)	-39.947(14)	21.810(6)	-10.635(3)	-1.311(3)	50	19.37
HNC	1024.9(1.4)	-18.59(4)	13.362(23)	-5.085(11)	-	40	14.91

Table 2: Isomerization barrier height in cm⁻¹ units for HCN and HNC computed from the bending energy functional (2DVM-I) and from the 2DVM optimized term values using Eq. (1) (2DVM-II) compared with results obtained using other approaches (columns third to fifth).

Molecule	E_{TS} comparison (cm ⁻¹)				
	2DVM-I	2DVM-II	Baraban <i>et al.</i> ³	Mourik <i>et al.</i> ³⁰	Makhnev <i>et al.</i> ³¹
HCN($\ell = 0$)	16580(50)	16570(30)	16695(17)	16798	16809.4
HNC($\ell = 0$)	11790(90)	11977(15)	11533(124)	11517	11496.6

An advantage of the algebraic model compared to a pure Dunham expansion is that it provides both the eigenvalues and also the eigenstates upon diagonalization of the Hamiltonian (2). The height of the isomerization barrier has strong consequences for the structure of the eigenstates and the dynamics of the HCN-HNC molecular system.^{32–34} Indeed, it has been recently shown that the system’s eigenstate with the closest energy to the saddle point that characterizes the transition state has an enhanced localization in the bending coordinates.⁴ A similar phenomenon has been discussed in the case of ESQPTs in different realizations of the vibron model, where eigenstates with eigenvalues close to the critical energy of the ESQPT have been shown to be localized in the basis associated with the linear configuration, also called the cylindrical oscillator basis.^{35–37}

The level of localization of states written in a certain basis can be quantified with the participation ratio (PR), as explained next. Hamiltonian (2) is block-diagonal in the vibrational angular momentum ℓ . Its eigenstates can be written as a linear combination of the cylindrical oscillator basis states $\{|[N]n^\ell\rangle\}$: $|\psi_k^{(\ell)}\rangle = \sum_n C_{k,n}^\ell |n^\ell\rangle$ and the participation ratio is defined as

$$\text{PR}(|\psi_k^{(\ell)}\rangle) = \left[\sum_n |C_{k,n}^\ell|^4 \right]^{-1}. \quad (3)$$

The minimum PR value is 1, when the system localization is maximal and the eigenstate can be identified with a basis state. The maximum PR value is the dimension of an ℓ -vibrational angular momentum basis block, which happens when all components are nonzero and have the same weight.

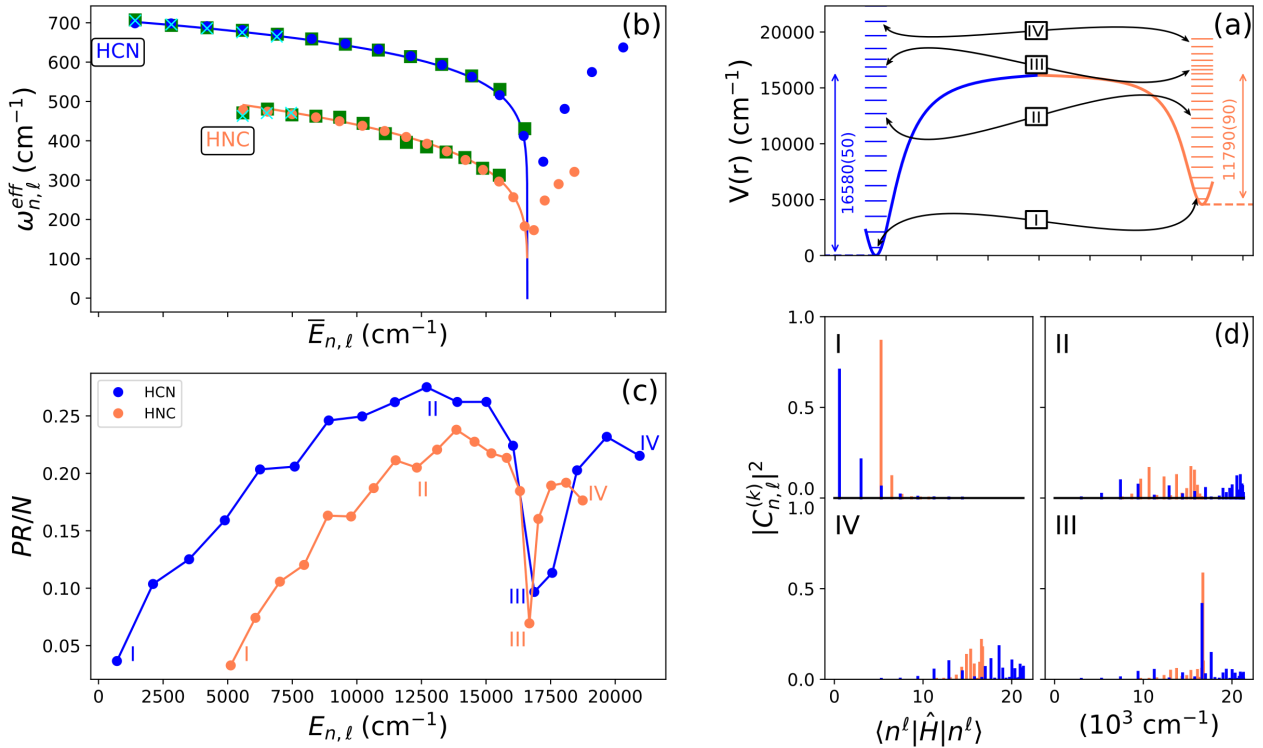


Figure 1: (Color online) Panel (a): sketch of the potentials obtained for the two molecular species using the intrinsic state formalism and the isomerization barrier values, locating the states I, II, III, and IV chosen to illustrate our results (see text). Panel (b): effective frequency $\omega_{n,\ell}^{\text{eff}}$ as a function of the midpoint excitation energy $\bar{E}_{n,\ell}$ for HCN and HNC. Crosses indicate the available experimental data, while green squares are spectroscopically assigned *ab initio* results (Ref.,⁵ see text). Blue (orange) circles are the algebraic model results and the blue (orange) line marks the result of fitting Eq. 1 to the algebraic fit results for HCN (HNC). Panel (c): Normalized participation ratio (see Eq. 3) of $\ell = 0$ HCN (blue dots) and HNC (orange dots) eigenstates resulting from the fit of the algebraic Hamiltonian (2) (See supplementary material for details) making use of a truncated cylindrical oscillator basis. Panels (d): Squared components in the cylindrical oscillator basis for four algebraic model eigenstates of HCN (blue bars) and HNC (orange bars) as a function of the expectation value of the Hamiltonian in the $|n^\ell\rangle$ basis state.

In the nonrigid case, the eigenstate at the ESQPT critical energy is strongly localized in the linear limit basis state with $n = 0$, a fact that affects the system dynamics by slowing down the evolution.^{35–38} The eigenstate at the isomerization barrier is also localized, but with a caveat, as we explain next. In the HCN-HNC case, we plot the PR for the $\ell = 0$

eigenstates normalized by the vibron number N in Fig. 1c with blue (orange) dots for HCN (HNC). In both cases, there is a remarkable decrease in the PR value for eigenstates close to the isomerization energy value. To further clarify the variation in the eigenstates structure, we include in Fig. 1a the two energy functional curves, and the energies of four states chosen to illustrate the different structures of the wave functions at different excitation energies. The four selected eigenstates of HCN and HNC, labeled as I , II , III , and IV , have energies at different locations in the PES: at the ground state energy, at a mid height, at the isomerization barrier, and above the barrier. The bar diagrams in the four panels of Fig. 1d are drawn from the squared value of the $C_{k,n}^\ell$ coefficients for those four eigenstates as a function of the energy of the corresponding basis vector, $\langle Nn^\ell | \hat{H} | Nn^\ell \rangle$; bars are blue (orange) for HCN (HNC) eigenstates. The change in the structure as we move from eigenstate I to IV is evident. The low energy eigenstate I is localized because the cylindrical oscillator basis is the most appropriate basis for the description of rigidly-linear configurations. Eigenstates II and IV are characterized by a strong mixing in the same basis. Eigenstate III is of special relevance, since it is the eigenstate with the closest energy to the isomerization barrier. It is characterized by a strong localization in a particular basis state. Contrary to what happens in the ESQPT for nonrigid molecules, where for $\ell = 0$ the basis element $|N0^0\rangle$ has the largest component,^{35–37} in the isomerization case, the minimum in the PR is associated to a large component in a basis state with a high n value, e.g. $|NN^0\rangle$ for an even N value. This is likely caused by anharmonicity effects in the Hamiltonian, as already hinted in.³⁹ Indeed, we verified that a negative quadratic contribution in the boson number operator has effects in the symmetric phase for linear and quasilinear states, before the control parameter reaches the critical value.

In short, we have thus shown that the 2DVM, despite the simplicity of the Hamiltonian (2), describes extremely well the localization and the effective frequency dip of the transition state for isomerizing systems, once it is fed with enough spectroscopic data or with accurate enough *ab initio* calculations. The value of the transition state energy can be estimated from

the intrinsic state energy functional or from the dip in the energy gap. In both cases the differences with the E_{TS} values obtained with sophisticated ab initio calculations are very small, around 1-2%. As a consequence of the link between the isomerization barrier and ESQPT's, our characterization of the transition state is not restricted to energy values and their differences only, but it includes also the structure of the algebraic wave function. This offers a promising line of research for applications of the ESQPT formalism in isomerization reactions.

The present approach also provides a physically sound way for obtaining a minimum bound for the vibron number value N , which needs to be large enough to accommodate the minimum in the participation ratio. Heretofore, in the case of bending vibrations, the value of the vibron number N used to be fixed based only on the best fit to experiment.²⁰

Finally, it is interesting to note that the 2DVM eigenstates with positive slope in the right end of Fig. 1b have energies beyond the isomerization energy barrier. Thus they cannot be unambiguously associated to one of the two molecular configurations and they correspond to the so-called bond-breaking states, which are often expressed with the $\text{H}_{0.5}\text{CNH}_{0.5}$ formula.³⁴ These eigenfunctions necessarily entangle both molecular configurations, something that in the 2DVM case was already noticed in Ref.²¹ (See Fig. 6 in this reference). A full description of the isomerizing HCN-HNC system at these energies requires the consideration of both molecules in a single system. This is a direction we plan to explore in the near future.

Acknowledgement

The authors thank Franco Iachello and José Miguel Arias for useful discussions and comments. JK thanks support from the Youth Employment Initiative and the Youth Guarantee program supported by the European Social Fund. LFS is supported by the NFS Grant No. DMR-1603418. This study has been partially financed by the Consejería de Conocimiento, Investigación y Universidad, Junta de Andalucía and European Regional Development Fund

(ERDF), ref. SOMM17/6105/UGR and by the Centro de Estudios Avanzados de Física, Matemáticas y Computación (CEAFMC) of the Universidad de Huelva. Computer resources supporting this work were provided by the CEAFMC and Universidad de Huelva High Performance Computer (HPC@UHU) located in the Campus Universitario el Carmen and funded by FEDER/MINECO project UNHU-15CE-2848.

Supporting Information Available

The following files are available free of charge.

The following files are available free of charge as supporting information.

- **Sup_Mat.pdf**: A brief explanation of the procedure followed to obtain the classical limit of the 2DVM and of the effective frequency fitting procedure. Results of the model for non-zero vibrational angular momentum.
- **SM_energies.txt**: Results obtained from the 2DVM fit to spectroscopically assigned *ab initio* energies including the comparison with experimental data when available.

References

- (1) Eyring, H. The Activated Complex in Chemical Reactions. *The Journal of Chemical Physics* **1935**, *3*, 107–115.
- (2) Wigner, E. The transition state method. *Trans. Faraday Soc.* **1938**, *34*, 29–41.
- (3) Baraban, J. H.; Changala, P. B.; Mellau, G. C.; Stanton, J. F.; Merer, A. J.; Field, R. W. Spectroscopic characterization of isomerization transition states. *Science* **2015**, *350*, 1338–1342.
- (4) Mellau, G. C.; Kyuberis, A. A.; Polyansky, O. L.; Zobov, N.; Field, R. W. Saddle point localization of molecular wavefunctions. *Sci. Rep.* **2016**, *6*, 33068.

(5) Harris, G. J.; Tennyson, J.; Kaminsky, B. M.; Pavlenko, Y. V.; Jones, H. R. A. Improved HCN/HNC linelist, model atmospheres and synthetic spectra for WZ Cas. *Mon. Not. R. Astron. Soc.* **2006**, *367*, 400–406.

(6) Mellau, G. C. Complete experimental rovibrational eigenenergies of HNC up to 3743cm-1 above the ground state. *J. Chem. Phys.* **2010**, *133*, 164303.

(7) Mellau, G. C. Complete experimental rovibrational eigenenergies of HCN up to 6880 cm-1 above the ground state. *J. Chem. Phys.* **2011**, *134*, 234303.

(8) Iachello, F. Algebraic methods for molecular rotation-vibration spectra. *Chem. Phys. Lett.* **1981**, *78*, 581 – 585.

(9) Iachello, F.; Oss, S. Algebraic approach to molecular spectra: Two dimensional problems. *J. Chem. Phys.* **1996**, *104*, 6956–6963.

(10) Iachello, F.; Pérez-Bernal, F.; Vaccaro, P. A novel algebraic scheme for describing nonrigid molecules. *Chem. Phys. Lett.* **2003**, *375*, 309 – 320.

(11) Pérez-Bernal, F.; Santos, L.; Vaccaro, P.; Iachello, F. Spectroscopic signatures of nonrigidity: Algebraic analyses of infrared and Raman transitions in nonrigid species. *Chem. Phys. Lett.* **2005**, *414*, 398 – 404.

(12) Dixon, R. N. Higher vibrational levels of a bent triatomic molecule. *Trans. Faraday Soc.* **1964**, *60*, 1363–1368.

(13) Child, M. S. Quantum states in a champagne bottle. *J. Phys. A: Math. Gen.* **1998**, *31*, 657–670.

(14) Pérez-Bernal, F.; Iachello, F. Algebraic approach to two-dimensional systems: Shape phase transitions, monodromy, and thermodynamic quantities. *Phys. Rev. A* **2008**, *77*, 032115.

(15) Gilmore, R.; Feng, D. Phase transitions in nuclear matter described by pseudospin Hamiltonians. *Nucl. Phys. A* **1978**, *301*, 189 – 204.

(16) Gilmore, R. The classical limit of quantum nonspin systems. *J. Math. Phys.* **1979**, *20*, 891–893.

(17) Cejnar, P.; Jolie, J.; Casten, R. F. Quantum phase transitions in the shapes of atomic nuclei. *Rev. Mod. Phys.* **2010**, *82*, 2155–2212.

(18) Cejnar, P.; Macek, M.; Heinze, S.; Jolie, J.; Dobeš, J. Monodromy and excited-state quantum phase transitions in integrable systems: collective vibrations of nuclei. *J. Phys. A* **2006**, *39*, L515.

(19) Caprio, M.; Cejnar, P.; Iachello, F. Excited state quantum phase transitions in many-body systems. *Ann. Phys.* **2008**, *323*, 1106 – 1135.

(20) Larese, D.; Iachello, F. A study of quantum phase transitions and quantum monodromy in the bending motion of non-rigid molecules. *J. Mol. Struct.* **2011**, *1006*, 611 – 628.

(21) Larese, D.; Pérez-Bernal, F.; Iachello, F. Signatures of quantum phase transitions and excited state quantum phase transitions in the vibrational bending dynamics of triatomic molecules. *J. Mol. Struct.* **2013**, *1051*, 310 – 327.

(22) Child, M. S.; Weston, T.; Tennyson, J. Quantum monodromy in the spectrum of H₂O and other systems: new insight into the level structure of quasi-linear molecules. *Mol. Phys.* **1999**, *96*, 371–379.

(23) Winnewisser, B. P.; Winnewisser, M.; Medvedev, I. R.; Behnke, M.; De Lucia, F. C.; Ross, S. C.; Koput, J. Experimental Confirmation of Quantum Monodromy: The Millimeter Wave Spectrum of Cyanogen Isothiocyanate NCNCS. *Phys. Rev. Lett.* **2005**, *95*, 243002.

(24) Zobov, N. F.; Shirin, S. V.; Polyansky, O. L.; Tennyson, J.; Coheur, P.-F.; Bernath, P. F.; Carleer, M.; Colin, R. Monodromy in the water molecule. *Chem. Phys. Lett.* **2005**, *414*, 193 – 197.

(25) Dietz, B.; Iachello, F.; Miski-Oglu, M.; Pietralla, N.; Richter, A.; von Smekal, L.; Wambach, J. Lifshitz and excited-state quantum phase transitions in microwave Dirac billiards. *Phys. Rev. B* **2013**, *88*, 104101.

(26) Zhao, L.; Jiang, J.; Tang, T.; Webb, M.; Liu, Y. Dynamics in spinor condensates tuned by a microwave dressing field. *Phys. Rev. A* **2014**, *89*, 023608.

(27) Winnewisser, M.; Winnewisser, B. P.; Medvedev, I. R.; Lucia, F. C. D.; Ross, S. C.; Bates, L. M. The hidden kernel of molecular quasi-linearity: Quantum monodromy. *J. Mol. Struct.* **2006**, *798*, 1 – 26.

(28) James, F.; Roos, M. MINUIT - System for function minimization and analysis of parameter errors and correlations. *Computer Physics Communications* **1975**, *10*, 343–367.

(29) Newville, M.; Stensitzki, T.; B. Allen, D.; Ingargiola, A. LMFIT: Non-Linear Least-Square Minimization and Curve-Fitting for Python. 2014.

(30) van Mourik, T.; Harris, G. J.; Polyansky, O. L.; Tennyson, J.; Császár, A. G.; Knowles, P. J. Ab initio global potential, dipole, adiabatic, and relativistic correction surfaces for the HCN–HNC system. *J. Chem. Phys.* **2001**, *115*, 3706–3718.

(31) Makhnev, V. Y.; Kyuberis, A. A.; Zobov, N. F.; Lodi, L.; Tennyson, J.; Polyansky, O. L. High Accuracy ab Initio Calculations of Rotational–Vibrational Levels of the HCN/HNC System. *J. Phys. Chem. A* **2018**, *122*, 1326–1343, PMID: 29251934.

(32) Bacic, Z.; Light, J. C. Accurate localized and delocalized vibrational states of HCN/HNC. *J. Chem. Phys.* **1987**, *86*, 3065–3077.

(33) Light, J. C.; Bacic, Z. Adiabatic approximation and nonadiabatic corrections in the discrete variable representation: Highly excited vibrational states of triatomic molecules. *J. Chem. Phys.* **1987**, *87*, 4008–4019.

(34) Mellau, G. C. Rovibrational eigenenergy structure of the [H,C,N] molecular system. *J. Chem. Phys.* **2011**, *134*, 194302.

(35) Santos, L. F.; Pérez-Bernal, F. Structure of eigenstates and quench dynamics at an excited-state quantum phase transition. *Phys. Rev. A* **2015**, *92*, 050101.

(36) Santos, L. F.; Távora, M.; Pérez-Bernal, F. Excited-state quantum phase transitions in many-body systems with infinite-range interaction: Localization, dynamics, and bifurcation. *Phys. Rev. A* **2016**, *94*, 012113.

(37) Pérez-Bernal, F.; Santos, L. F. Effects of excited state quantum phase transitions on system dynamics. *Progr. Phys. Fortschr. Phys.* **2017**, *65*, 1600035.

(38) Kloc, M.; Stránský, P.; Cejnar, P. Quantum quench dynamics in Dicke superradiance models. *Phys. Rev. A* **2018**, *98*, 013836.

(39) Pérez-Bernal, F.; Álvarez-Bajo, O. Anharmonicity effects in the bosonic U(2)-SO(3) excited-state quantum phase transition. *Phys. Rev. A* **2010**, *81*, 050101.